Robotica: (2020) volume 38, pp. 639–651. © Cambridge University Press 2019
doi:10.1017/S0263574719000912

Longitudinal Regrasping of Elongated Objects

Avishai Sintov†*, Or Tslil‡ and Shahar Frenkel‡

†*Coordinated Science Laboratory, University of Illinois at Urbana-Champaign, Urbana, IL 61801, USA*
‡*Department of Mechanical Engineering, Ben-Gurion University of the Negev, Beer-Sheva, 84105, Israel*
E-mails: ortslil64@gmail.com, shaharf131@gmail.com

(Accepted May 25, 2019. First published online: July 31, 2019)

SUMMARY
Regrasping is a manipulation to alternate between grasp configurations of an object to perform different tasks. We address a regrasping problem termed *longitude regrasping* to reposition a gripper along an elongated object. We propose an algorithm using the dynamics of the arm and a non-dexterous gripper to perform the manipulation. Energy control is used to toss the object up and catch it under the goal position. Clipped Linear Quadratic Regulator control approach is then applied to the gripper jaws to control the friction force on the object and to let it slide to the final goal position. The object sliding within the gripper is modeled as a semi-active linear joint where only dissipative forces can be applied to it. A set of experiments validated the feasibility of the method.

KEYWORDS: Regrasping; Elongated objects; Dynamic manipulations.

1. Introduction

Different tasks on the same object require altering between grasp configurations. Such alternation is termed *regrasping*[1] and is widely researched in the robotics community with a large interest in bioinspired mimic of the human motion. Current robotic regrasping methodologies work only with highly redundant (and hence expensive) hand architectures, and require overly sophisticated sensory feedback. In this paper, we use the dynamics of the robotic arm and a simple non-dexterous gripper to address a sector of the regrasping problem termed *longitudinal regrasping*. Such regrasping manipulation is designated for elongated objects where the aim is to reposition the gripper along the object. This can be done by dynamic manipulation to achieve fast regrasping, that is, tossing to midair or sliding along the object. Humans perform longitude regrasping when holding long rods, spears, bottles, etc., to improve grasping posture or to perform different tasks. Herons, for example, perform similar manipulation for a better grip of their prey. In this work, we wish to mimic such dynamic regrasping manipulation.

This work was motivated by the redundant use of robotic arms in industrial production lines. In production lines, there are many versatile robotic arms that can be used for various tasks. However, an end effector mounted on an arm is specifically designed to hold a specific part for a specific task at a specific station along the line. Thus, the robotic arm is limited to a specific task. Regrasping using a single robot arm and a non-dexterous end effector offers an attractive solution in terms of cost as well as task completion time. In addition, a versatile manipulation should be as independent as possible of external resources such as obstacles to push against. Thus, the robot can be reused by performing regrasping based on the tasks to be done. In this paper, we combine various methods presented in our previous work[2,3] and is a natural extension. We combine different techniques used separately before as novel means to perform the regrasping task. We prioritize and propose to use standardizations in

* Corresponding author. E-mail: avishai.sintov@gmail.com

https://doi.org/10.1017/S0263574719000912 Published online by Cambridge University Press

our algorithms. By doing so, it is simple to generalize algorithms for different motions. This work is part of a larger research theme that aims to create a library of dynamic regrasping capabilities implemented with generic tools. Thus, we can generalize different tasks in the higher level and simplify future decision algorithms. A general algorithm would be able to choose between different motions and use generic tools to autonomously perform various tasks.

In the robotics literature, there are four known approaches for regrasping. The first approach is picking and placing where the object is put on a surface and picked up again in a different grasp configuration.[4,5] The pick and place approach is rather slow and demands a large area in the vicinity of the robot. The second approach is the use of an additional robotic arm to regrasp – this is known as *dual-arm* regrasping and manipulations.[6] While dual-arm regrasping is a promising approach, it has two significant drawbacks. First, regrasping an object with two cooperating arms require highly dexterous manipulation capabilities from both arms. Second, a dual-arm system is costly and occupies a fairly large work volume.

The third approach is the use of the gripper's degrees of freedom (DOFs) to move between contact points while maintaining a force-closure grasp during the entire process.[7–10] This approach is also called *quasi-static finger gaiting* in the robotics literature. However, quasi-static finger gaiting can be wasteful, as it requires sufficiently many DOFs (requiring highly redundant finger mechanism) to manipulate the grasped object between two grasp configurations while maintaining force closure grasps. Using more DOFs can be a problem in terms of cost, of recovery from failure if one motor breaks, and of control complexity. The fourth approach is much faster and efficient, however more complex, as it uses dynamical manipulations to switch between grasp configurations. The end effector allows relative velocity (by throwing or sliding) with the object through a series of dynamic manipulations.[11–14] Some work done in this field use a multi-fingered highly dexterous hand for performing regrasping. The work of Furukawa et al.[15] proposed a regrasping strategy based on the visual feedback of the manipulated object, with a multi-fingered hand. Tahara et al.[16] introduced a regrasping method using a three-finger hand with no external sensing for feedback.

In this paper, we propose an algorithm based on energy and Linear Quadratic Regulator (LQR) control methods to perform the longitude regrasping. The energy control[17,18] is aimed to gain the grasped object with the necessary energy. Energy control would enable the object to be tossed, reach the desired goal position with zero velocity and be caught by the gripper below the desired position. This replaces regular tossing in a desired initial velocity by adding feedback and overcoming model inaccuracies. Further, a simple gripper holding the object and allowing it to slide within it acts as a *semi-active linear joint*.[19,20] The notion of a semi-active joint arises from semi-active friction dampers[21] to control the normal force and improve performance compared to passive dampers. Such joint is able only to resist the motion of the object; that is, it can only dissipate energy. This is done by controlling the normal force applied to the object by the grippers jaws to vary the friction forces while it slides within the gripper. To refine the grasp and accurately bring it to the goal position, a modified LQR control[22] is used, termed *clipped* LQR (cLQR).[23] The cLQR provides a control signal for a positive normal force to be applied to the object to complete the regrasping.

2. Problem Definition

In this section, we present the longitudinal regrasping problem and formulate it analytically. We begin with the manipulator dynamics as follows. Consider n-joint manipulator given by

$$D(\mathbf{q})\ddot{\mathbf{q}} + C(\mathbf{q}, \dot{\mathbf{q}})\dot{\mathbf{q}} + G(\mathbf{q}) = \mathbf{u_m} \tag{1}$$

where $\mathbf{q}(t) = [q_1(t) \cdots q_n(t)]^T \in \mathbb{R}^n$ is the vector of joints angles at time t, $\mathbf{u_m}(t) = [u_1(t) \cdots u_n(t)]^T \in \mathbb{R}^n$ is the torque control vector, D is an $n \times n$ inertia matrix, C is the $n \times n$ centrifugal and Coriolis matrix, and G is an $n \times 1$ vector of joint torques due to gravitational force. A simple jaw gripper is fixed at the tip of link n. Both jaws of the gripper are parallel such that they can apply parallel and equal forces $f_N \geq 0$ to the grasped object.

Given an elongated object with length L and unknown mass m held by the gripper (Fig. 1), let e be the object axis along L containing its center of mass (COM). We set the motion of the arm such that the gripper and object move only parallel to gravity. That is, e is parallel to gravity during the manipulation. Nevertheless, misalignment of e could be tolerated due to the catch of the object below the desired goal in the tossing phase as will be described later on. Moreover, we assume that

https://doi.org/10.1017/S0263574719000912 Published online by Cambridge University Press

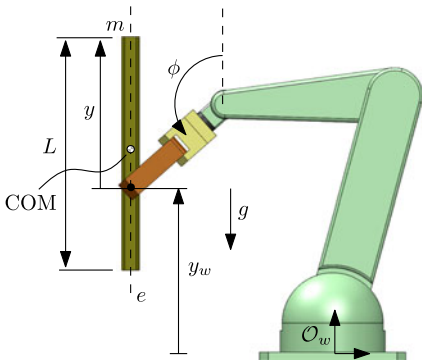


Fig. 1. An elongated object gripped by the robotic arm.

the contact points are always on e such that the COM is always directly above or below it. We discuss the means to remove this assumptions in the Conclusions section. Let y be the position of the object top edge relative to the grippers contact points such that $y = 0$ is when the gripper holds the top point and $y = L$ is grasping the bottom. Moreover, let $\mathcal{O}_w$ be the manipulator's coordinate frame fixed at the base and y_w be the height of the gripper relative to $\mathcal{O}_w$.

The regrasping problem is defined as follows. An object is held by the gripper of system (1). Given the initial position $y(t = 0) = y_o$ between the object and the gripper, perform a manipulation motion such that

$$\lim_{t\to\infty} y(t) = y_d \ , \quad \lim_{t\to\infty} \dot{y}(t) = 0 \tag{2}$$

In other words, the manipulation motion should bring the gripper to position y_d with zero velocity. We measure the state of the object $\mathbf{x} = (y\ \dot{y})^T$ during the manipulation.

3. Model Formulation

3.1. Object model

In this work, it was not dealt with the motion planning of the arm, hence its ability was assumed to generate acceleration of the gripper in any direction. Nevertheless, as mentioned, the motion of the gripper is performed only on the vertical axis. Moreover, throughout the motion of the gripper, the pitch angle ϕ (see Fig. 1) of the gripper is maintained constant to avoid undesired dynamic effects on the object.

Two models for the object are defined and used in different phases of the motion. When the object is fixed to the gripper, they both accelerate together and therefore the gripper and objects equation of motion is given by

$$\ddot{y}_w = a \tag{3}$$

where a is the vertical acceleration input applied by the gripper. When the gripper is stationary, that is, $\dot{y}_w = 0$, and relative velocity between the gripper and object is possible, the object's equation of motion is

$$m\ddot{y} + mg = f \tag{4}$$

where f is the frictional force exerted on the object. Therefore, the object has two inputs: acceleration a provided by the motion of the arm and friction force f defined by the normal force f_N applied by the gripper. The frictional model is presented next.

3.2. Friction model

Friction exists between the gripper's jaws and the object. We assume the Coulomb friction model[24] between the jaws and objects surfaces. When there is no relative velocity (i.e., $\dot{y} = 0$), static friction force f_s is exerted at the contact point

$$|f_s| \leq \mu f_N \tag{5}$$

https://doi.org/10.1017/S0263574719000912 Published online by Cambridge University Press

where $\mu > 0$ is the static coefficient of friction assumed to be known. When relative velocity exists, $\dot{y} \neq 0$, we use the *Signum-Friction Model*[25] expressing the friction force as

$$f_m = -\nu f_N \text{sgn}(\dot{y}) \tag{6}$$

where $\nu > 0$ is the dynamic coefficient of friction. Note that f_m is a dissipative force and therefore has opposite direction to motion. For changing velocities where the velocity crosses the $\dot{y} = 0$ line, switching between models (5) and (6) leads to numerical difficulties. Karnopp[26] proposed to define a small neighborhood of zero velocity, $|\dot{y}| \leq \varepsilon$ for some small $\varepsilon > 0$, where the friction force f is equal to the net force f_t acting on the object. To maintain zero velocity, the normal force f_N will be chosen to counterbalance the net force with $f_N = |f_t|/\mu$. The overall friction model used in this work defines the friction force f with respect to the normal force as

$$f(f_N) = \begin{cases} -\mu f_N \text{sgn}(f_t), & |\dot{y}| \leq \varepsilon \\ -\nu f_N \text{sgn}(\dot{y}), & |\dot{y}| > \varepsilon \end{cases} \tag{7}$$

One may view the system of the arm and object as an under-actuated $(n+1)$-DOF arm with n fully actuated joints and one semi-actuated[21] linear joint. A semi-actuated joint enables only to counteract the motion by controlling the normal force applied at the contact point. That is, we apply a positive normal force while the resultant tangential force must satisfy the dissipative constraint

$$f \cdot \dot{y} < 0 \tag{8}$$

The control of such joints imposes difficulties as a control force cannot be applied to assist in the direction of motion and it must constantly satisfy (8).

While accelerating the gripper with a, we would like the object to remain fixed to it. Hence, it is required to apply sufficient normal force to avoid slippage. In other words, the friction force must satisfy $f \geq ma - mg$ and therefore, using (5), the gripper must apply normal force satisfying

$$f_N \geq \frac{1}{\mu}|ma - mg| \tag{9}$$

During the acceleration, the gripper must update the normal force to satisfy (9).

4. Method

Assuming that the goal position has higher potential energy than the initial grasp, the regrasping motion is divided into two phases. The first phase is based on energy control to lift up the object relative to the gripper, that is, to increase the object energy and bring it to the vicinity of the desired goal. In simple words, the object is tossed straight up and grasped under the desired goal position. Catching the object exactly at the desired position is very hard and demands highly accurate hardware. Therefore, we catch below the desired position with an offset λ. Thus, this phase can overcome large errors and inaccuracies. The first phase ends at time t_c. In the second phase, the object is accurately brought to the final grasp while the gripper is stationary. We use cLQR to control the normal force and let the object slide in the gripper to the final position. If the goal position has lower potential energy than the initial, the algorithm will skip to the second phase. The theories of energy control and cLQR are discussed next followed by the final process for performing the regrasping manipulation.

4.1. Energy control

Controlling the object's energy is an efficient way to bring it near the desired goal position. Assume an initial configuration such that the object at initial grasp has lower potential energy than the goal. We use the arm and gripper to provide the object with enough kinetic energy to reach the goal's potential energy. Once the gripper and object reached the necessary energy, the object is released. After the release, the object is thrown up until all kinetic energy transforms into the desired potential energy where it is caught again by the gripper. This format enables catching the object at the desired position with zero velocity.

The energy of the object is given by

$$E(h, \dot{h}) = \frac{1}{2}m\dot{h}^2 + mgh \tag{10}$$

https://doi.org/10.1017/S0263574719000912 Published online by Cambridge University Press

where h is the height of the object relative to some reference point. The initial and goal energies of the object relative to the gripper are $E_o = E(y_o, 0)$ and $E_d = E(y_d, 0)$, respectively. Before releasing the object, we would like the kinetic energy of the gripper to be equal to the required energy difference, or in other words we require

$$E_d = E_o + E(0, \dot{y}_w) \tag{11}$$

Hence, the energy of the object–gripper system is given by the right side of the equation and is equal to $E(y_o, \dot{y}_w)$. Furthermore, its change rate is given by the derivative of (10):

$$\dot{E}(y_0, \dot{y}_w) = m\dot{y}_w\ddot{y}_w \tag{12}$$

By substituting (3) in (12), we get

$$\dot{E}(y_0, \dot{y}_w) = m\dot{y}_w a \tag{13}$$

This means, as expected, that increasing or decreasing the objects energy could be done using a. Thus, we would like to find a control law for a that will give the object energy to reach E_d. The next theorem proposes such controller and is based on ref. [27].

Theorem 1. *Let $E(y_o, \dot{y}_w)$ be the energy of the system at time t. The control law*

$$a = -\Gamma\,(E - E_d)\,\dot{y}_w \tag{14}$$

with some user defined gain $\Gamma > 0$, will increase the object's energy to E_d.

Proof. Consider the following Lyapunov candidate function[27]

$$V = \frac{1}{2}\,(E - E_d)^2 \tag{15}$$

where $E = E(y_o, \dot{y}_w)$. Substituting (13) to the time derivative of V gives

$$\dot{V} = (E - E_d)\,\dot{E} = (E - E_d)\,m\dot{y}_w a \tag{16}$$

By applying controller (14)–(16), we show that

$$\dot{V} = -m\Gamma\dot{y}_w^2\,(E - E_d)^2 \leq 0 \tag{17}$$

Therefore, as long as $\dot{y}_w \neq 0$, the Lyapunov function decreases and the systems energy is driven to E_d. □

Control law (14) will drive the object to the desired energy E_d. When starting from rest, the velocity is zero and therefore the controller could not be initiated. Hence, we apply initial velocity at time $t = 0$ toward the goal. Otherwise the energy control would move in the wrong direction. Therefore, we use an impact function

$$a(0) = \delta \tag{18}$$

where δ is a user-defined value. Note that the impact value must be larger than g to overcome the object's mass and initiate motion.

We have shown stability of controller (14) only in the energy domain, not in the state space. That is, the motion will remain on a manifold in the state space defined by $E(y_o, \dot{y}_w) = E_d$. The object would converge to the desired energy but not to the desired state. Therefore, once the system reaches the desired energy, the gripper would release the object so it can change its position relative to the gripper. With the acquired energy, the object will reach the desired height with zero velocity, making it easier to catch. The sequence of actions will be presented later.

4.2. Clipped LQR control

We first examine the stabilization of a fully actuated linear joint, that is, with an actuator not obligated to the dissipation constraint (8). In this phase, the gripper is stationary and we consider the system in (4) in the state-space form

https://doi.org/10.1017/S0263574719000912 Published online by Cambridge University Press

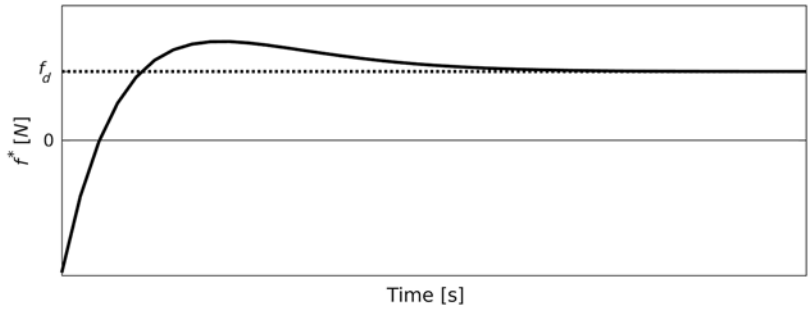


Fig. 2. Optimal force input on a fully actuated linear joint.

$$\dot{\mathbf{x}} = \mathbf{f}(\mathbf{x}, f) = \begin{pmatrix} x_2 \\ m^{-1}(f - mg) \end{pmatrix} \tag{19}$$

where $\mathbf{x} = (x_1\ x_2)^T = (y\ \dot{y})^T$ is the state of the object relative to the gripper and $f = f(f_N)$ is the friction force controlled with the normal force input according to (7). We wish to stabilize the system on $\mathbf{x_d} = (y_d\ 0)^T$. Further, the desired force f_d to hold the object stationary at $\mathbf{x_d}$ must satisfy $\mathbf{f}(\mathbf{x_d}, f_d) = 0$, which yields the gravity resisting force $f_d = mg$. Therefore, we define the error state $\mathbf{x_e} = \mathbf{x} - \mathbf{x_d}$ and the input error $f_e = f - f_d$. Linearization of the system around $(\mathbf{x_d}, f_d)$ yields the linear time-invariant continuous-time system

$$\dot{\mathbf{x}}_e(t) = A\mathbf{x_e}(t) + Bf_e(t) \tag{20}$$

where

$$A = \begin{bmatrix} 0 & 1 \\ 0 & 0 \end{bmatrix},\ B = \begin{pmatrix} 0 \\ m^{-1} \end{pmatrix} \tag{21}$$

and $\mathbf{x_e}(t_c) = \mathbf{x}(t_c) - \mathbf{x_d}$ is the initial condition. We define a quadratic cost function of the form

$$J(\mathbf{x_e}) = \int_{t_c}^{\infty} \left(\mathbf{x_e}^T Q \mathbf{x_e} + R f_e^2\right) dt \tag{22}$$

with $Q = Q^T \geq 0$ and $R > 0$ as weighting matrices. This provides an optimal feedback control[28]

$$f_e^* = -R^{-1}B^T P\mathbf{x_e} = -K\mathbf{x_e} \tag{23}$$

where P is the solution of the Riccati equation

$$Q - PBR^{-1}B^T P + PA + A^T P = 0 \tag{24}$$

The cost-to-go of the optimal control policy is

$$J^*(\mathbf{x_e}) = \mathbf{x_e}^T P\mathbf{x_e} \tag{25}$$

From (23), the optimal feedback control which would be applied to (4) would be

$$f^* = -K(\mathbf{x} - \mathbf{x_d}) + f_d \tag{26}$$

Note that the controllability matrix $\mathcal{C}$ of system (20) with control (23), that is, $\dot{\mathbf{x}}_e(t) = (A - BK)\mathbf{x_e}(t)$, is non-singular – the system is controllable.[29] The control law in (26) applied to the joint could provide force in both up and down directions, with no regards to the dissipative constraint in (8). While the object slides down ($\dot{y} < 0$), negative force is applied to assist the object followed by positive force to slow down the object to the goal force f_d (Fig. 2). The negative forces do not satisfy (8) and demand negative normal force from the gripper, a demand which cannot be provided. In terms of controllability, although $\mathcal{C}$ remains full rank, the availability of only positive forces means that some states cannot be formed by a linear combination of the columns of $\mathcal{C}$. That is, the system is now uncontrollable. Thus, only forces in one direction can be applied and the tossing phase is

https://doi.org/10.1017/S0263574719000912 Published online by Cambridge University Press

required. Consequently, the controller should be modified to force $f^* \geq 0$, or equivalently, $f_N \geq 0$. From (26), demanding $f^* \geq 0$ means

$$\dot{y} \leq \frac{1}{k_2}(f_d - k_1(y - y_d)) \tag{27}$$

where k_1 and k_2 are the components of the gain vector K. Condition (27) defines a region of attraction to initiate optimal controller (26). If the condition is not satisfied, the object is allowed to slide in the gripper with gravity and with a minimal friction force f_{min}. Therefore, the control signal from (26) is clipped, and the modified cLQR controller[21] has the form

$$f(t > t_c) = \begin{cases} f^*, & \dot{y} \leq \frac{1}{k_2}(f_d - k_1(y - y_d)) \\ f_{min}, & \text{otherwise} \end{cases} \tag{28}$$

The desired normal force to be applied in order to acquire $f(t > t_c)$ is calculated according to (7).

4.3. Regrasping algorithm

The full process for performing longitude regrasping from an initial position y_o to the goal position y_d is presented next. First, we check whether the energy of the initial grasp is higher than the goal. If so, the cLQR controller can be applied directly. Otherwise, the object is first tossed up using the energy control and caught in a point under the goal. Then, the cLQR can be applied. As mentioned, the aim of the energy control phase is to bring the gripper to grasp the object under the desired position. This addition compensates for object misalignment, friction loss, model inaccuracies, inaccurate release, and motion of the gripper after release until full stop. Thus, the user defines the offset length λ below the desired position y_d. Then, a new intermediate goal position y'_d is calculated along with its compatible potential energy E'_d.

After defining the control gain and impact magnitude, we apply an initial impact $a(0)$ as defined in (18) for a small time interval $\Delta t \ll 1$ s. Next, the control energy law (14) is implemented while measuring the object's state to close the control loop. Once the object reaches the desired energy E'_d, the object is released with a minimal friction force f_{min} and the gripper is braked. Then, when the object reaches instant halt and satisfies $|\dot{y}| \leq \varepsilon$, it is caught by applying a large normal force. The final step is to allow the object to slide in the gripper to position using cLQR controller (28). The next section presents a simulation to demonstrate the method followed by a set of experiments.

5. Simulations

Simulations were performed on a 3-DOF robotic arm. Videos of the simulations can be seen in Extension 1. An $L = 0.4$ m length Polyvinyl Chloride (PVC) bar with mass of $m = 0.156$ kg is initially grasped at position $y_o = 0.05$ m. The aim is to regrasp the bar at a final position $y_d = 0.2$ m. The PVC bar is simulated to slide within rubber jaws having frictional coefficient of $\mu = 0.85$ and $\nu = 0.8$. In addition, zero velocity as presented in (7) is defined by $\varepsilon = 0.005$. In the first phase of the energy control, the goal position was defined with an offset of $\lambda = 0.1$ m under the original goal, that is, $y'_d = y_d + \lambda = 0.3$ m. The initial impulse was set to $\delta = 10$ and the control gain was set to $\Gamma = 40$. In the second phase, the LQR cost functions weighting matrices were chosen manually to be $Q = diag([5 \cdot 10^3 \ 10^2])$ and $R = 1$ in order to prioritize smooth motion. Consequently, this yielded a control gain vector of $K = (70.7 \ \ 11.04)$. With this K and by substituting (23) in (20), the closed loop system is now

$$\dot{\mathbf{x}}_e(t) = (A - BK)\mathbf{x_e}(t) = \tilde{A}\mathbf{x_e}(t) = \begin{bmatrix} 0 & 1 \\ -453.27 & -70.82 \end{bmatrix} \mathbf{x_e}(t) \tag{29}$$

The eigenvalues of $\tilde{A}$ are -7.11 and -63.7 yielding a stable system if the contact joint was fully actuated.

Figure 3 shows snapshots of the simulated bar to regrasp it at the new desired position. The position response can be seen in Fig. 4 showing both position $y(t)$ relative to the gripper and absolute position $y(t) + y_w(t)$ relative to $\mathcal{O}_w$. It can be seen that the object did not fully reached y'_d due to friction loss. The energy response of the bar is seen in Fig. 5. The energy controller operates until it reaches the desired energy E'_d at time $t = 0.91$ s. Free flight occurs until time $t_c = 1.12$ s when the object reaches near the desired position y'_d with zero velocity. At that time instant, the gripper is

https://doi.org/10.1017/S0263574719000912 Published online by Cambridge University Press

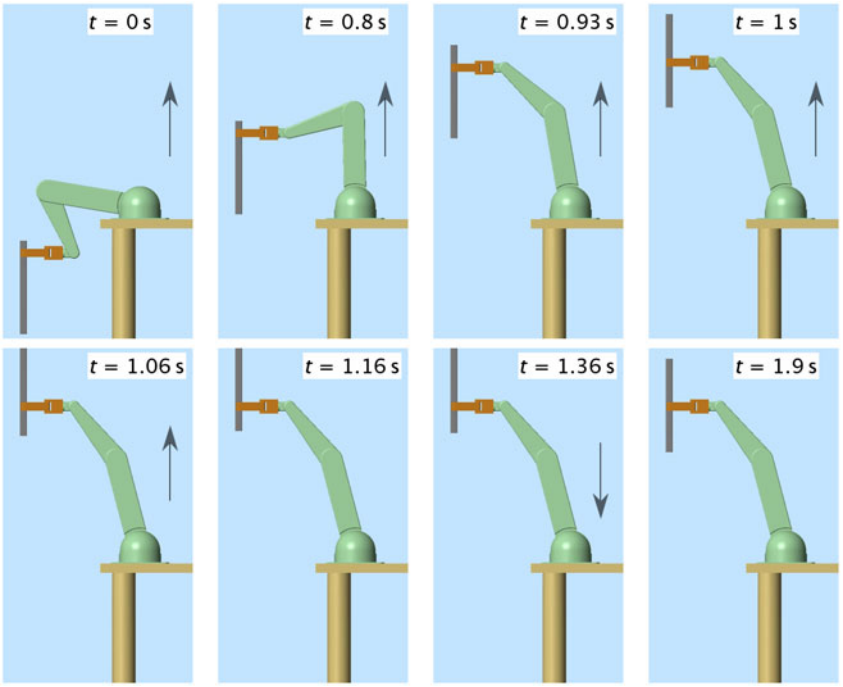


Fig. 3. Simulation of the longitude regrasping from $y_0 = 0.05$ [m] to $y_d = 0.2$ [m]. The arrow indicates the object's direction of motion.

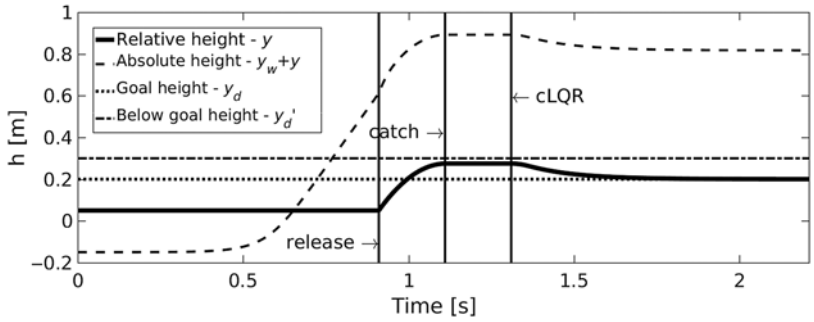


Fig. 4. The object's height response. The solid curve indicates the height y relative to the gripper while the dashed curve is the height $y_w + y$ relative to $\mathcal{O}_w$.

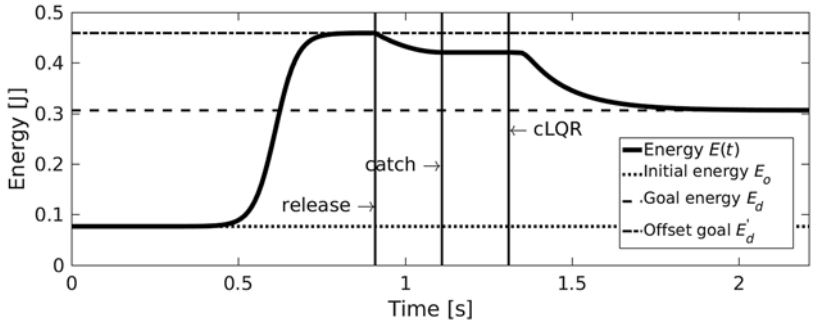


Fig. 5. The object's energy response.

instantly closed to catch the object. From $t = 1.32$ s, the cLQR acts to let the bar slide in the gripper to the desired position y_d.

Figure 6 illustrates the two inputs to the bar. Figure 6(a) shows the acceleration a of the gripper. Acceleration a begins with large intensity for tossing up the bar to increase its energy. At time $t =$

https://doi.org/10.1017/S0263574719000912 Published online by Cambridge University Press

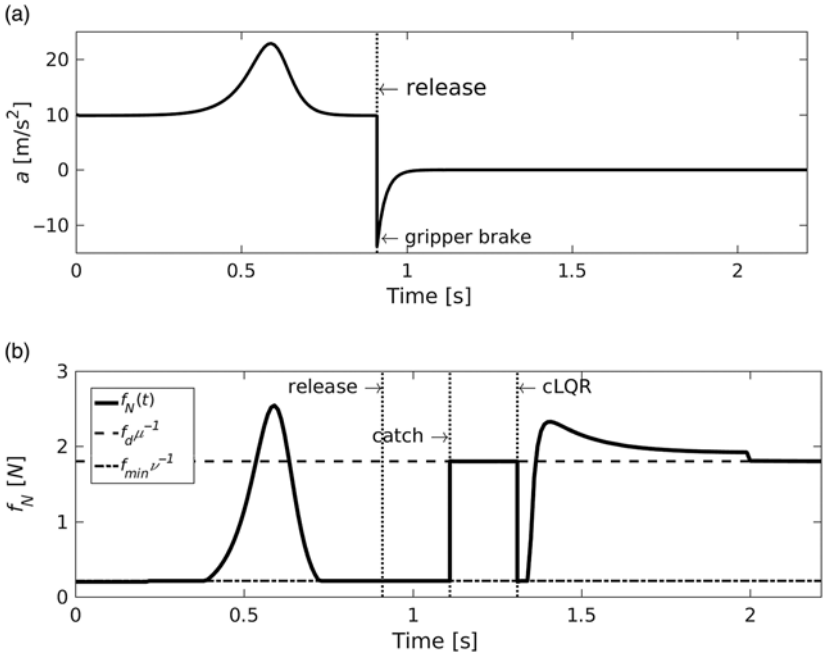


Fig. 6. (a) Acceleration input to the pivot of the object and (b) normal force applied to the bar by the gripper.

0.91 s, right after the release of the object, the gripper is braked. The negative peak at that time is the deceleration of the gripper. The effect on the bar is minimal as the friction force f_{min} is very small. In Fig. 6(b), the normal force applied on the bar is seen. A relatively high normal force is necessary before release to prevent slipping due to the accelerations. After catch, the friction force equals the gravity force of the bar and then lowered by the cLQR to allow slippage to position. At the end of the slippage, the friction force returns to be equal to the gravity in order to maintain the bar at the goal position. The small discontinuity at time 2 s is the transition from dynamic friction to static according to (7).

6. Experiments

To show the feasibility of the proposed regrasp method, we have conducted several experiments presented in this section. A video of the experiments can be seen in the supplementary material.

6.1. ROS–Gazebo experiment

For preliminary tests of the proposed algorithm, we have built a 7R KUKA iiwa robotic arm in a realistic Robot Operating System (ROS)–Gazebo environment. The joints were position controlled using PID controllers. Initially, the gripper holds an elongated cylinder with length $L = 0.4$ m at point $y_o = 0.052$ m. The goal of the manipulation is to regrasp the object at its middle, that is, $y_d = 0.2$ m. Snapshots of the experiments can be seen in Fig. 7 and the relative position response at Fig. 8. At time $t = 1.81$ s, the energy controller is initiated, operated until release at time $t = 2.22$ s. At time $t_c = 2.41$ s, the cylinder is caught below the desired position at $y'_d = 0.27$ m. At time $t = 0.35$ s, the cLQR is initialized leading the cylinder to its final desired position.

6.2. Full regrasping experiment

To fully test the algorithm, we have built an experimental setup. A two-jaw gripper was built using two parallel Robotis MX-106R Dynamixel actuators. These actuators were chosen due to their ability to receive torque commands and therefore apply the desired normal forces on the bar. A metal plate was mounted on each motor and 3D printed fingers were fixed to the jaws opposing each other. The fingers are fixed such that when the jaws are set parallel to each other, the facets of the fingers are parallel as well and the distance between them can be varied using screws. The gripper was mounted on a 6-DOF Robotis Manipulator-H composed of six Dynamixel-Pro actuators (Fig. 9). Both the arm and gripper were controlled using the ROS.

https://doi.org/10.1017/S0263574719000912 Published online by Cambridge University Press

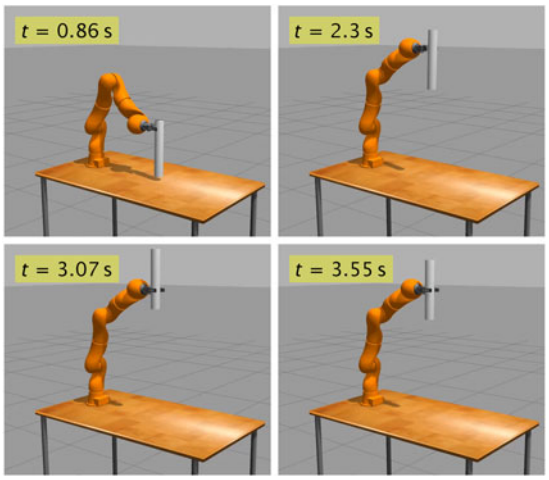


Fig. 7. An experiment with a KUKA arm performing longitudinal regrasping of a cylinder in ROS–Gazebo.

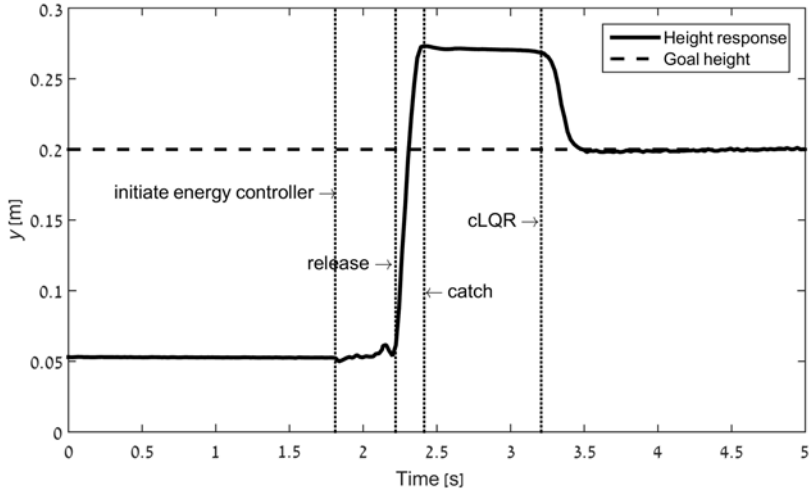


Fig. 8. The height response between the KUKA's gripper and the cylinder.

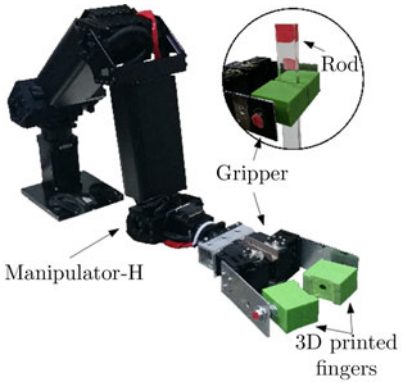


Fig. 9. The Robotis Manipulator-H experimental setup.

The sliding object was selected to be a polymethyl methacrylate (PMMA) bar with length $L = 0.35$ m and mass $m = 0.058$ kg. The coefficients of friction between the printed fingers and bar were measured to be $\nu = 0.39$ and $\mu = 0.404$. Distance y was measured in real time with an RGB camera and the velocity was calculated by backward finite difference of second-order accuracy. Preliminary

https://doi.org/10.1017/S0263574719000912 Published online by Cambridge University Press

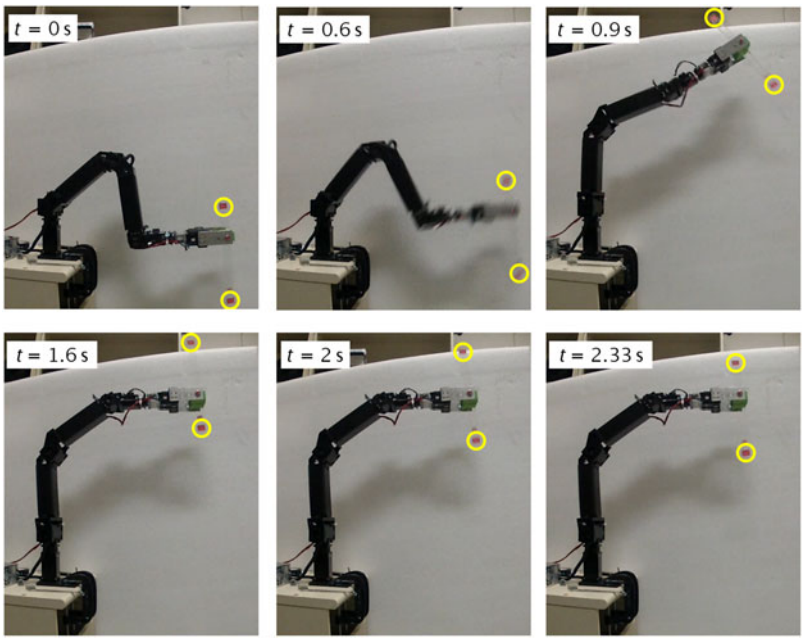


Fig. 10. Snapshots of the Manipulator-H arm performing a longitude regrasping. The ends of the bar are marked with yellow circles.

testing of the semi-active linear joint control was conducted and can be seen in the supplementary video.

We present a regrasping experiment where the goal was to regrasp the bar from position $y_o = 0.09$ m to $y_d = 0.11$ m. The additional offset was chosen to be $\lambda = 0.07$ m and the energy control gain was set to $\Gamma = 260$. The cLQR controller was implemented with $Q = diag([5 \times 10^4 \ 10^3])$ and $R = 1$ resulting in a control gains vector of $K = (223.6 \ \ 32.3)$. Snapshots of the regrasping are shown in Fig. 10. In high velocities, the synchronization between the arm's actuators performed poorly and therefore the gripper did not move solely along on the y_w-axis with constant pitch angle of 90°. Nevertheless, this phase, as discussed in Section 4.3, is not planned to be accurate but only position the gripper somewhere below the desired pose. Thus, the addition of λ enabled to accomplish the manipulation. Before the sliding, the object was positioned in its vertical pose followed by the cLQR sliding.

The position response can be seen in Fig. 11. The bar reached $y = 0.108$ m close to the desired goal with a small error of 1.1 mm. It should be noted that due to noisy signal readings from the camera and actuators, a simple mean filter was applied for noise reduction. The small dent around time $t = 0.6$ s is due to a minor slippage of the bar while accelerating the gripper. In that time instant, the acceleration is in its peak and the dynamixel actuators of the gripper reached saturation. Nevertheless, the slippage was minor and did not interfere with the manipulation. The acceleration and energy responses can also be seen in Fig. 11. Five experiments were conducted in total with different start and goal configurations resulting in average displacement error of 1.7 mm.

7. Conclusions

In this paper, we have presented an algorithm for performing longitude regrasping. The algorithm used energy control to toss the object so it can reach a point below the desired goal with zero velocity. After catching it, cLQR controller is applied to let the object slide within the gripper to the desired final position. An important aspect of the algorithm is the modeling of the sliding object as a semi-active linear joint. Such model is suitable for applying optimal control and then clipping it to ensure satisfying the dissipative constraint. We have shown experiments on a Manipulator-H arm performing the longitude regrasping from release using energy control to stabilization using cLQR. Despite the technical difficulties in the real-robot experiment, the robot was able to toss the object and slide it into position. The experiment yielded similar and expected behavior compared to the simulations. They

https://doi.org/10.1017/S0263574719000912 Published online by Cambridge University Press

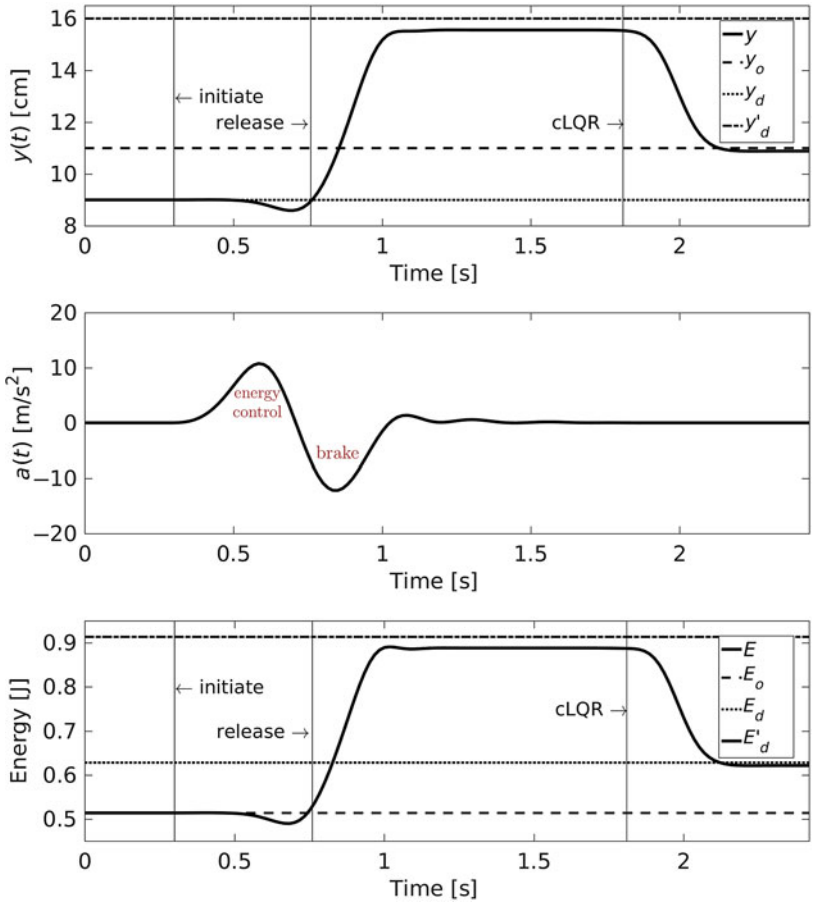


Fig. 11. Experimental results of the (top) bar's relative position y response, (middle) the grippers acceleration a, and (bottom) energy response while regrasping.

exhibited matching responses. Therefore, both simulations and experiments validated the proposed algorithm.

In the work, we have made an assumption that the COM of the object must be above or below the contact points. Such assumption can be overcome by maintaining controlled friction through contact with the object to prevent it from tilting. Alternatively, integrating a control method[13] can compensate tilting of the object due to misalignment. A control method can also act to balance the object at the same orientation. We leave this for future work.

The presented approach is restricted to the particular motion due to the design of the gripper. In future work, we would consider extended control methods to remove the restriction and allow the arm to perform a set of motions. Further, although the proposed approach can overcome model inaccuracies, it is model based. The human hand, for instance, does not know in advance the dynamic properties of the manipulated object but manages to approximate them right before performing a successful manipulation. In addition, real-time interferes from the environment and uncertainties such as nonuniform friction and delayed actions are difficult to model. Thus, we view the proposed method as preliminary understanding of the manipulation and will seek for a more adaptive and general approach in the future. Future work will address the planning and control of such manipulations in real-world environments where the robot should adapt and fix its actions on the fly. Future work could also deal with heavy objects where the energy controller reaches saturation. In such case, the algorithm should be modified to perform several tosses before applying the cLQR controller.

Supplementary Material

To view supplementary material for this article, please visit https://doi.org/10.1017/S0263574719000912.

https://doi.org/10.1017/S0263574719000912 Published online by Cambridge University Press

References

1. A. A. Cole, P. Hsu and S. S. Sastry, "Dynamic control of sliding by robot hands for regrasping," *IEEE Trans. Robot. Auto.* **8**(1), 42–52 (1992).
2. A. Sintov and A. Shapiro, "Swing-Up Regrasping Using Energy Control," *Proceedings of the IEEE International Conference on Robotics and Automation (ICRA)*, Stockholm, Sweden (2016).
3. A. Sintov, O. Tslil and A. Shapiro, "Robotic swing-up regrasping manipulation based on impulse-momentum approach and cLQR control," *IEEE Trans. Robot.* **32**(5), 1079–1090 (2016).
4. J.-P. Saut, M. Gharbi, J. Cortes, D. Sidobre and T. Simeon, "Planning Pick-and-Place Tasks with Two-Hand Regrasping," *Proceedings of IEEE/RSJ International Conference on Intelligent Robots and Systems*, Taipei, Taiwan (2010) pp. 4528–4533.
5. P. Tournassoud, T. Lozano-Perez and E. Mazer, "Regrasping," *Proceedings of IEEE International Conference on Robotics and Automation*, Raleigh, NC, USA, vol. 4 (1987) pp. 1924–1928.
6. B. Balaguer and S. Carpin, "Bimanual Regrasping from Unimanual Machine Learning," *Proceedings of IEEE International Conference on Robotics and Automation*, Saint Paul, MN, USA (2012) pp. 3264–3270.
7. B. Corves, T. Mannheim and M. Riedel, "Re-grasping: Improving capability for multi-arm-robot-system by dynamic reconfiguration," **In:** *Intelligent Robotics and Applications*, vol. 7101 (Springer, Berlin, Heidelberg, 2011) pp. 132–141.
8. M. A. Roa and R. Suarez, "Regrasp Planning in the Grasp Space Using Independent Regions," *Proceedings of IEEE/RSJ International Conference on Intelligent Robots and Systems, IROS'09*, St. Louis, MO, USA (2009) pp. 1823–1829.
9. M. Stuheli, G. Caurin, L. Pedro and R. Siegwart, "Squeezed screw trajectories for smooth regrasping movements of robot fingers," *J. Brazilian Soc. Mech. Sci. Eng.* **35**(2), 83–92 (2013).
10. P. Vinayavekhin, S. Kudoh and K. Ikeuchi, "Towards an Automatic Robot Regrasping Movement Based on Human Demonstration Using Tangle Topology," *Proceedings of IEEE International Conference on Robotics and Automation*, Shanghai (2011) pp. 3332–3339.
11. N. Dafle, A. Rodriguez, R. Paolini, B. Tang, S. Srinivasa, M. Erdmann, M. Mason, I. Lundberg, H. Staab and T. Fuhlbrigge, "Regrasping Objects Using Extrinsic Dexterity," *Proceedings of IEEE International Conference on Robotics and Automation*, Hong Kong (2014) p. 2560.
12. Y. Hou, Z. Jia, A. M. Johnson and M. T. Mason, "Robust Planar Dynamic Pivoting by Regulating Inertial and Grip Forces," *Workshop on the Algorithmic Foundations of Robotics*, San Francisco, CA, USA (2016).
13. A. Sintov and A. Shapiro, "Dynamic regrasping by in-hand orienting of grasped objects using non-dexterous robotic grippers," *Robot. Comput. Integ. Manufact.* **50**, 114–131 (2018).
14. K. Hang, M. Li, J. A. Stork, Y. Bekiroglu, F. T. Pokorny, A. Billard and D. Kragic, "Hierarchical fingertip space: A unified framework for grasp planning and in-hand grasp adaptation," *IEEE Trans. Robot.* **32**(4), 960–972 (2016).
15. N. Furukawa, A. Namiki, S. Taku and M. Ishikawa, "Dynamic regrasping using a high-speed multifingered hand and a high-speed vision system," *Proceedings of IEEE International Conference on Robotics and Automation*, Orlando, FL, USA (2006) pp. 181–187.
16. K. Tahara, K. Maruta, A. Kawamura and M. Yamamoto, "Externally Sensorless Dynamic Regrasping and Manipulation by a Triple-Fingered Robotic Hand with Torsional Fingertip Joints," *Proceedings of IEEE International Conference on Robotics and Automation*, Saint Paul, MN, USA (2012) pp. 3252–3257.
17. X. Xin, S. Tanaka, J. H. She and T. Yamasaki, "Revisiting Energy-Based Swing-Up Control for the Pendubot," *Proceedings of the IEEE International Conference on Control Applications*, Yokohama (2010) pp. 1576–1581.
18. K. Astrom and K. Furuta, "Swinging up a pendulum by energy control," *Automatica* **36**(2), 287–295 (2000).
19. J. S. Lane and A. A. Ferri, "Optimal Control of a Semi-Active, Frictionally Damped Joint," *American Control Conference*, Chicago, IL, USA (1992) pp. 2754–2759.
20. L. Gaul, H. Albrecht and J. Wirnitzer, "Semi active friction damping of large truss structures," *Shock and Vibration* **11**(3), 173–186 (2004).
21. P. Dupont, P. Kasturi and A. Stokes, "Semi-active control of friction dampers," *J. Sound Vibrat.* **202**, 203–218 (1997).
22. K. Ogata, *Modern Control Engineering* (Prentice-Hall, Englewood Cliffs, NJ, 1998).
23. K. Popp, A. Guran and F. Pfeiffer, *Dynamics with Friction: Modeling, Analysis and Experiment*, *EBL-Schweitzer* (World Scientific Publishing, 2001).
24. R. M. Murray, Z. Li and S. S. Sastry, *A Mathematical Introduction to Robotic Manipulation*, 1st edn. (CRC Press, Boca Raton, FL, USA, 1994).
25. L. Gaul and R. Nitsche, "The role of friction in mechanical joints," *ASME Appl. Mech. Rev.* **54**(2), 93–106 (2001).
26. D. Karnopp, "Computer simulation of stick-slip friction in mechanical dynamic systems," *ASME. J. Dyn. Sys. Meas. Control* **107**(1), 100–103 (1985).
27. S. Durand, F. Guerrero Castellanos, N. Marchand and W. F. Guerrero Sánchez, "Event-based control of the inverted pendulum: Swing up and stabilization," *J. Control Eng. Appl. Inf.* **15**(3), 96–104 (2013).
28. R. Tedrake, I. R. Manchester, M. Tobenkin and J. W. Roberts, "LQR-trees: Feedback motion planning via sums-of-squares verification," *Int. J. Rob. Res.* **29**(8), 1038–1052 (2010).
29. H. Trentelman, A. A. Stoorvogel and M. Hautus, *Control Theory for Linear Systems*, 1st edn. (Springer-Verlag, London, UK, 2001).

https://doi.org/10.1017/S0263574719000912 Published online by Cambridge University Press